

# Flame Studies of Conventional and Alternative Jet Fuels

Chunsheng Ji,\* Yang L. Wang,\* and Fokion N. Egolfopoulos<sup>†</sup>  
University of Southern California, Los Angeles, California 90089

DOI: 10.2514/1.B34105

**Laminar flame speeds and extinction limits of premixed and nonpremixed flames of conventional jet fuels, such as jet propellant 7 and jet propellant 8, and alternative jet fuels, such as synthetic and bioderived, were determined in the counterflow configuration at atmospheric pressure and elevated unburned reactant temperature. The results were compared against those of flames of *n*-decane and *n*-dodecane, both being candidate components of jet fuel surrogates. Results indicate that jet propellant 8/air and jet propellant 7/air flames exhibit lower propagation speeds and resistance to extinction compared with flames of alternative fuels. The reduced reactivities of jet propellant 8/air and jet propellant 7/air flames are caused by the alkylcycloparaffins and alkylbenzenes that are present in notable quantities in conventional jet fuels. The combustion characteristics of bioderived jet fuels were found to be indistinguishable from those produced synthetically via the Fischer–Tropsch process. The phenomena of flame propagation and extinction were modeled using *n*-decane and *n*-dodecane flames, for which kinetic models are available and for which the molecular weight is representative of that of practical jet fuels. Sensitivity analysis was performed, and results revealed that, compared with flame propagation, flame extinction is, in general, more sensitive to kinetics and diffusion, especially under nonpremixed conditions.**

## I. Introduction

DESPITE their extensive use in airbreathing propulsion, the combustion properties of conventional petroleum-derived jet fuels, such as jet propellant 7 (JP-7) and jet propellant 8 (JP-8), are still not well characterized. JP-7 and JP-8 fuels contain myriads of compounds, with compositions that are variable and dominated by *n*-paraffins, isoparaffins, cycloparaffins, and aromatics compounds (e.g., [1]). The oxidative and pyrolytic characteristics of these classes of fuels are known to differ notably and, as a result, the combustion characteristics of JP-7 and JP-8 are sensitive to fuel composition variations.

In addition, the trend of fuel diversification is expected to continue and accelerate, especially with respect to fuels derived from renewable sources, such as biomass, and those produced synthetically via, for example, the Fischer–Tropsch (F–T) process [2]. Currently, F–T and bioderived fuels are considered as alternative fuels in airbreathing propulsion. Examples of F–T fuels are those derived from natural gas by Syntroleum, hereafter referred to as S-8, and from gas to liquid (GTL) by Shell, hereafter referred to as Shell-GTL. An example of a bioderived fuel is that produced by Tyson from animal/vegetable oil and subsequently deoxygenated, hereafter referred to as R-8. These three fuels are available to researchers, and it has been reported that they have similar compositions<sup>‡</sup> that are dominated by *n*-paraffins and isoparaffins [3]. Although the viability of the S-8, Shell-GTL, and R-8 fuels has been demonstrated in military aircraft, their chemical and physical properties have yet to be fully characterized (e.g., [4]).

The large number of complex hydrocarbons present in conventional and synthetic jet fuels makes their modeling a rather daunting task. Thus, recent and current efforts have been focusing on developing suitable surrogate fuels that could be modeled. However, deriving surrogate fuels that can closely mimic both the physical and chemical properties of practical jet fuels over a wide range of conditions remains a major challenge. Compared with neat

compounds, few studies exist on the combustion characteristics of conventional and alternative jet fuels. Different experimental methodologies, such as flow reactors [5,6], shock tubes [7,8], and spherical [9] and counterflow flames [10–14], have been used to measure the ignition delay times, laminar flame speeds, and extinction limits of conventional and alternative jet fuels over wide ranges of temperatures and pressures. Although many efforts have focused on the development of pertinent kinetic models (e.g., [15–23]), there still exists notable disagreement among experimental data, as well as between experiments and models predictions.

Based on the aforementioned considerations, the main goal of this study is to provide archival experimental data on flame propagation and extinction of JP-7/air, JP-8/air, S-8/air, Shell-GTL/air, and R-8/air flames, which will contribute toward better understanding of their high-temperature combustion characteristics. Laminar flame speeds  $S_u^o$  and extinction strain rates  $K_{ext}$  of premixed and nonpremixed flames were determined in the counterflow configuration for a wide range of equivalence ratios  $\phi$ . All measurements were carried out at atmospheric pressure and elevated fuel-carrying stream temperatures  $T_u$ . The data obtained in premixed flames were compared against those obtained for *n*-decane ( $n\text{-C}_{10}\text{H}_{22}$ ) and *n*-dodecane ( $n\text{-C}_{12}\text{H}_{26}$ ) flames in a previous study by the Ji et al. [24]. Measurements of  $K_{ext}$  of nonpremixed  $n\text{-C}_{10}\text{H}_{22}$  and  $n\text{-C}_{12}\text{H}_{26}$  flames were performed in this study as well. The compounds  $n\text{-C}_{10}\text{H}_{22}$  and  $n\text{-C}_{12}\text{H}_{26}$  have molecular weights that are similar to JP-7 ( $\text{C}_{12}\text{H}_{25}$ ) and JP-8 ( $\text{C}_{11}\text{H}_{21}$ ) [1], as well as S-8 ( $\text{C}_{10}\text{H}_{22.7}$ ) [2], and they are among the main candidate components of jet fuel surrogates (e.g., [20]). The molecular weights of Shell-GTL and R-8 fuels are not available, and they were assumed to be close to that of S-8, given that their chemical compositions are similar.<sup>‡</sup>

## II. Experimental Approach

### A. General Configuration and Procedures

$S_u^o$  were determined in the symmetric twin-flame opposed-jet configuration, as shown schematically in Fig. 1 (e.g., [24–28]). The extinction studies of premixed flames involved the use of the single-flame configuration that results from counterflowing an ambient temperature  $\text{N}_2$  jet against a heated fuel/air jet [24]. The single premixed flame configuration was chosen over the twin-flame one, as it results in lower  $K_{ext}$ , compared with the twin-flame configuration. Lower  $K_{ext}$  require lower Reynolds numbers (generally between 400 and 1500), so that intrinsic flow instabilities are minimized.

Received 7 September 2010; revision received 15 December 2010; accepted for publication 30 January 2011. Copyright © 2011 by the American Institute of Aeronautics and Astronautics, Inc. All rights reserved. Copies of this paper may be made for personal or internal use, on condition that the copier pay the \$10.00 per-copy fee to the Copyright Clearance Center, Inc., 222 Rosewood Drive, Danvers, MA 01923; include the code 0748-4658/11 and \$10.00 in correspondence with the CCC.

\*Graduate Research Assistant, Department of Aerospace and Mechanical Engineering.

<sup>†</sup>Professor, Department of Aerospace and Mechanical Engineering. Senior Member AIAA.

<sup>‡</sup>Tim Edwards, private communications, 2008.

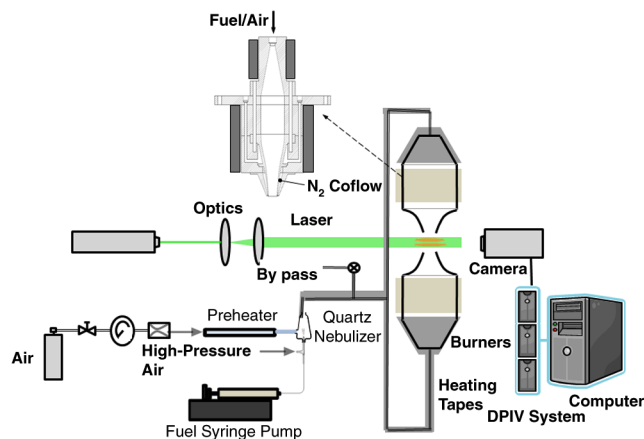


Fig. 1 Schematic of the experimental configuration.

Nonpremixed flames were established by counterflowing an ambient temperature  $O_2$  jet against a heated fuel/ $N_2$  jet [12]. Different burner nozzle diameters  $D$  and nozzle separation distances  $L$  were used. More specifically,  $D = L = 14$  mm was used for the determination of  $S_{u,ref}^o$ , while,  $D = L = 10$  mm was used for the determination of  $K_{ext}$ .

The vaporization system included a high-precision syringe pump to inject the liquid fuel [24]. Uniformly sized fuel droplets, ranging from 0.5 to 5  $\mu m$ , were produced with a nebulizer (Meinhard, type TR-50-C3), and they were vaporized instantly in a vaporization chamber. To prevent fuel condensation, the gas delivery line was wrapped with heating tape and the temperature was monitored using  $K$ -type unsheathed thermocouples. The partial pressure of the fuel was kept below its vapor (saturation) pressure under all conditions reported in this work. The burners were heated with ceramic heating jackets. A  $K$ -type thermocouple was used to monitor  $T_u$  at the center of the burner exit. All measurements were performed at  $p = 1$  atm and  $T_u = 403$  K.

The axial flow velocities were measured along the stagnation streamline using digital particle image velocimetry (DPIV). The flow was seeded with submicron-sized droplets of silicon oil that was previously mixed with the fuel at small concentrations, i.e., 0.2 ~ 0.5%. The vaporization temperature of the silicon oil is 540 K, which allows the droplets to survive well into the preheat zone while capturing the minimum point of the axial velocity profile just upstream of the flame that is defined as a reference flame speed  $S_{u,ref}$ , as shown schematically in Fig. 2. The droplets are small enough so that they follow the flow and they have no measurable effect on the flames [12]. A dual laser head, Solo neodymium-doped-yttrium-

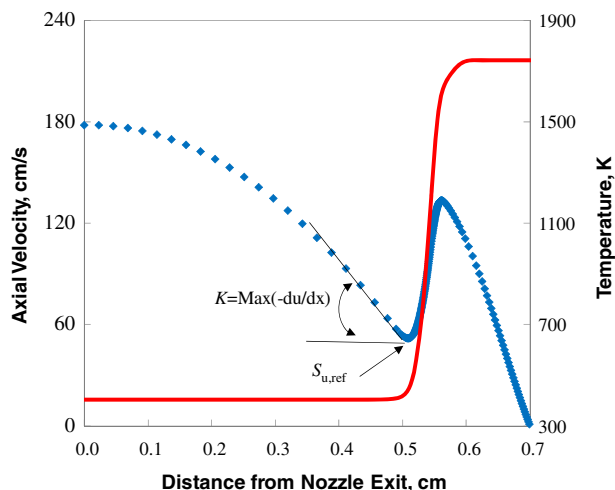


Fig. 2 Typical computed axial velocity profile along system centerline and definitions of  $K$  and  $S_{u,ref}$  (symbols: velocity profile; and line: temperature profile).

aluminum-garnet laser system (New Wave Research, type Solo-III-15) was used in this work. This laser system produces a 50 mJ/pulse light beam at 532 nm, with a 3–5 ns pulse width and a 3.5 mm beam diameter. A particle image velocimetry imager intense system (LaVision) was used to capture the images. The system contains a 12-bit 1376  $\times$  1040-pixel charge-coupled device (CCD) camera (pixel size 6.45  $\times$  6.45  $\mu m$ ), which runs at 5 frames/s, along with a 200 mm/F4 Micro Nikkor lens, a PC interface board, and a programmable timing unit (version 9) for generation of complex patterns of pulses with highly accurate timing controlled by the DPIV software. An optical filter with a passband centered at 532 nm was used to minimize the luminous emission from the flames. The CCD camera operates at a double frame mode that records the first frame with 10  $\mu s$  exposure, while the second image was integrated for 100 ms. The DPIV software is capable of recording the image data as well as processing them through the cross-correlation data reduction technique.

$S_{u,ref}^o$  is determined experimentally by first establishing the variation of  $S_{u,ref}$  with the strain rate  $K$ , which is defined as the absolute value of the maximum velocity gradient, as shown in Fig. 2 as well. Subsequently, the variation of  $S_{u,ref}$  with  $K$  is computed using a detailed description of chemical kinetics and molecular transport. Additionally,  $S_{u,ref}^o$  is computed and corresponds to  $K = 0$ . The computed  $S_{u,ref}$  and  $S_{u,ref}^o$  values are then fitted as a polynomial function of  $K$ . This polynomial function could then be translated vertically to best fit the experimental  $S_{u,ref}$  and determine  $S_{u,ref}^o$ . This computationally assisted nonlinear extrapolation is described in detail in previous studies by Ji et al. [24], Wang et al. [29], and Veloo et al. [30]. It has been shown [24,29,30] that small but finite uncertainties in rate constants and reactant transport coefficients have a negligible effect on the shape of the nonlinear  $S_{u,ref}$  vs  $K$  correlation, which can thus be used with confidence to determine  $S_{u,ref}^o$  from the raw experimental data. All raw experimental data (i.e., the variation of  $S_{u,ref}$  vs  $K$ ) in this study were well documented and are available upon request. The JetSurF 1.0 kinetic model [31] was used to produce the  $S_{u,ref}$  vs  $K$  correlations and attendant polynomial fits for  $n$ -C<sub>10</sub>H<sub>22</sub> and  $n$ -C<sub>12</sub>H<sub>26</sub> flames at conditions that are identical to those considered in the jet fuel flames. Given that reliable surrogate fuels and the attendant kinetic models are not available for jet fuels, the polynomial functions derived from  $n$ -C<sub>10</sub>H<sub>22</sub> flames were also used to fit the experimental  $S_{u,ref}$  of JP-7, JP-8, S-8, Shell-GTL, and R-8 flames; details of the JetSurF 1.0 kinetic model will be given in Sec. III.

Similar to  $S_{u,ref}^o$ ,  $K_{ext}$  cannot be measured directly. Its determination requires that a near-extinction flame be established first, followed by a measurement of the prevailing  $K$  just upstream of the flame. Subsequently, the fuel flow rate in the fuel/air jet is varied slightly to achieve extinction [24,28]. In premixed flame experiments for fuel-lean mixtures, this is done by slightly reducing the fuel flow rate, while for fuel-rich mixtures, extinction is achieved by slightly increasing the fuel flow rate. For nonpremixed flames, slight reduction of fuel in the fuel/ $N_2$  stream results in extinction. The modification to  $K$  due to the small changes in the fuel flow rate has been determined to be insignificant.

The U.S. Air Force Research Laboratory has provided the four jet fuels with attendant POSF identification numbers, and their compositions are summarized in Table 1. JP-7 (POSF-3327) consists mainly of  $n$ -paraffins, isoparaffins, cycloparaffins, and a small amount of aromatics (less than 1%). JP-8 (POSF-3773) contains  $n$ -paraffins, isoparaffins, and cycloparaffins, as well as notable amounts of aromatics (greater than 13%). The compositions of two F-T fuels [S-8 (POSF-4734) and Shell-GTL (POSF-5172)], however, are dominated by  $n$ -paraffins and isoparaffins, with negligible amounts of cycloparaffins and aromatics being present. The composition of R-8 (POSF-5469) is reported to be similar to S-8<sup>2</sup> and is not shown in Table 1.

## B. Experimental Uncertainties

The uncertainties of the experimentally determined  $S_{u,ref}$ ,  $S_{u,ref}^o$ , and  $K$  are attributed largely to the uncertainties associated with the

**Table 1** Jet fuel composition on a per mass basis

	JP-7 (POSF-3327)	JP-8 (POSF-3773)	S-8 (POSF-4734)	Shell-GTL (POSF-5172)
Paraffins ( <i>n</i> - + iso-)	67.9	57.2	99.7	99.0
Cycloparaffins	21.2	17.4	<0.2	0.8
Dicycloparaffins	9.4	6.1	<0.1	<0.1
Tricycloparaffins	0.6	0.6	<0.1	<0.1
Alkylbenzenes	0.7	13.5	<0.1	<0.1
Others	0.2	5.2	<0.1	<0.1

flowfield and the DPIV measurements. The fluctuation of  $T_u$  affects the density of the unburned gas and the nozzle exit velocity. In this work,  $T_u$  was measured at the center of the burner exit, and it was found to vary by as much as  $\pm 2$  K. Although this fluctuation is small, its influence was accounted for by making a linear correction to  $S_{u,ref}^o$  using a simple density scaling relation. The upstream pressure of each sonic orifice was monitored by a pressure gauge with a precision of  $\pm 0.25\%$ . For the liquid fuel injection rate, the syringe pump has a reported accuracy of  $\pm 0.5\%$ . The uncertainty associated with the DPIV measurements can be estimated by considering various parameter settings, such as the period between pulses, pixel resolution, and timing error [32]. Using the estimation method reported in [32], the DPIV uncertainty is determined to be within the range of 0.8 to 1.0%. The combined uncertainty can then be estimated using the following equation [33]:

$$u_c(y) = \sqrt{\sum_{i=1}^n \left( \frac{df}{dx_i} \right)^2 u^2(x_i)} \quad (1)$$

in which  $u_c(y)$  is the combined standard uncertainty of the measurand  $y$  ( $S_{u,ref}$  and  $K$  in this study),  $u(x_i)$  is the uncertainty of the measurable quantities  $x_i$  ( $T_u$ ,  $\phi$ , and measurement error of DPIV in this study), and  $y = f(x_1, x_2, \dots, x_n)$  is their mathematical relationship. The  $df/dx_i$  gradient is a measure of the sensitivity of function  $f$  with respect to quantity  $x_i$ . In the current study, all the measurable quantities are assumed to be uncorrelated, so there is no covariance term in Eq. (1). Moreover, most of the sensitivity coefficients,  $df/dx_i$ , in this study are considered to be unity. For example, perturbing 1% of the pressure gauge value will also change the oxidizer flow rate by 1%. Thus, the combined standard uncertainty of the velocity measurements can be estimated to be 1.25% using Eq. (1).

Figure 3 depicts the histograms of the experimentally determined  $K$  and  $S_{u,ref}$  under a given air/fuel flow rate. In Fig. 3,  $\bar{K}$  is the mean strain rate and  $\sigma(\bar{K})$  is the standard deviation, defined as  $\sqrt{\sum_{i=1}^N (K_i - \bar{K})^2 / (N - 1)}$ ;  $\bar{S}_{u,ref}$  is the mean reference flame speed and  $\sigma(\bar{S}_{u,ref})$  is the standard deviation, defined as

$\sqrt{\sum_{i=1}^N (S_{u,ref,i} - \bar{S}_{u,ref})^2 / (N - 1)}$ , where  $N$  is the total number of data sets. A total number of 150 data sets were recorded. Both  $K$  and  $S_{u,ref}$  exhibit a normal distribution, as shown in Fig. 3. The standard deviations for  $K$  and  $S_{u,ref}$  are 1.3 and 1.2%, respectively, which are close to the estimated values. It should be noted that the uncertainty of  $K_{ext}$  is the same as that of  $K$ , while the uncertainty of  $S_u^o$  is not the same as that of  $S_{u,ref}$ , given that  $S_u^o$  is an extrapolated value.

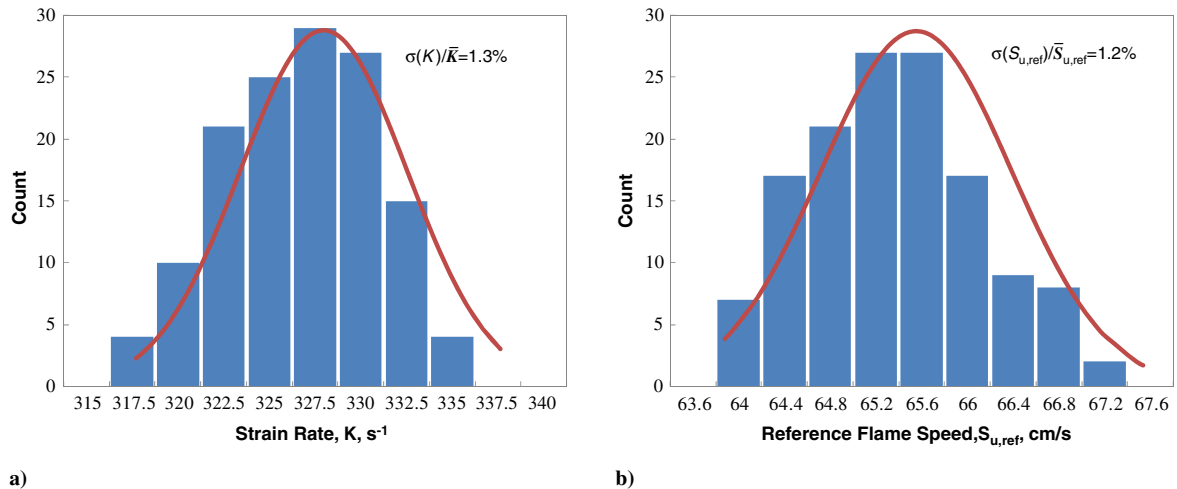
Figure 4 depicts the measured  $S_{u,ref}$  as a function of  $K$  for JP-7/air flames at  $\phi = 1.0$ . There exists a minimum value of  $K$  below which measurements are not possible, given that the flames become unstable and, eventually, flashback occurs. It is noticed that, for Karlovitz numbers  $Ka$ , defined as  $K\delta/S_u^o$  (where  $\delta$  is a characteristic flame thickness), are greater than 0.015, the variation of  $S_{u,ref}$  with  $K$  is nearly linear ( $120 \text{ s}^{-1} < K < 480 \text{ s}^{-1}$ ). As  $Ka$  approaches zero, a nonlinear behavior is noted. The uncertainty of  $S_u^o$ ,  $\varepsilon(S_u^o)$  could then be estimated using the following equation [34]:

$$\varepsilon(S_u^o) = \pm t_{(\alpha/2)}^{(N-2)} s \sqrt{1 + \frac{1}{N} + \frac{\bar{K}^2}{\sum_{i=1}^N (K_i - \bar{K})^2}} \quad (2)$$

where  $N$  is the total number of data sets,  $t_{(\alpha/2)}^{(N-2)}$  is the critical value of  $t$  distribution having  $N - 2$  degrees of freedom with a  $100(1 - \alpha)\%$  confidence interval, and  $s$  is the standard error of the estimated  $S_u^o$  defined as

$$s = \sqrt{\frac{\sum_{i=1}^N (S_{u,ref,i} - \bar{S}_{u,ref})^2}{N - 2}} \quad (3)$$

where  $S_{u,ref,i}$  is the reference flame speed of the  $i$ th measurement, and  $S_{u,ref,i}$  is the calculated reference flame speed at strain rate  $K_i$  using the polynomial function fitted by the nonlinear extrapolation methodology. The variables  $\varepsilon(S_u^o)$  are estimated to be  $\pm 1 \sim 2$  cm/s for the conditions used in this work. Figure 4 also depicts the upper [ $S_u^o + \varepsilon(S_u^o)$ ] and lower [ $S_u^o - \varepsilon(S_u^o)$ ] prediction limits, as well as  $S_u^o$ , for a stoichiometric JP-7/air flame with a 95% ( $\alpha = 0.05$ ) confidence interval.

**Fig. 3** Histograms of a)  $K$  and b)  $S_{u,ref}$  at a given air/fuel flow rate for JP-7/air flames at  $\phi = 1.0$ .

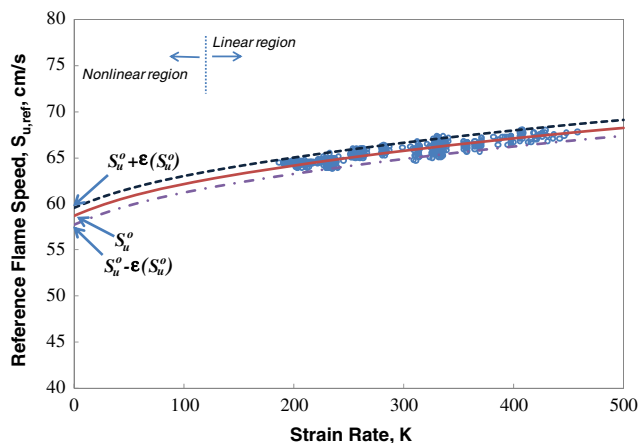


Fig. 4 Determination of  $S_u^0$  for a stoichiometric JP-7/air flame at  $p = 1$  atm and  $T_u = 403$  K (○: experimental data; solid lines: nonlinear extrapolation; dashed line: upper prediction limit; and dashed-dotted line: lower prediction limit).

### III. Modeling Approach

Given that reliable surrogate fuels and the attendant kinetic models are not currently available, computations of  $S_u^0$  and  $K_{\text{ext}}$  were carried out for  $n\text{-C}_{10}\text{H}_{22}$  and  $n\text{-C}_{12}\text{H}_{26}$  flames in order to provide insight into the phenomena of flame propagation and extinction for jet fuels. The compounds  $n\text{-C}_{10}\text{H}_{22}$  and  $n\text{-C}_{12}\text{H}_{26}$  were used as representative fuels, because their molecular weights are similar to jet fuels and notable amounts of  $n$ -paraffins are present in all jet fuels. At the same time, it should be noted that by considering either  $n\text{-C}_{10}\text{H}_{22}$  or  $n\text{-C}_{12}\text{H}_{26}$ , essentially as a one-component surrogate, several effects are missing, stemming from the oxidation of isoparaffins, cycloparaffins, and aromatics. At the same time, it is of interest to quantify the effect of omitting the aforementioned compounds on flame propagation and extinction that are indicative of the heat release rate in flames.

$S_u^0$  and  $K_{\text{ext}}$  were computed, respectively, using the PREMIX code [35,36] and an opposed-jet flow code [37] that was originally developed by Kee et al. [38]. Both codes have been modified to account for thermal radiation of  $\text{CH}_4$ ,  $\text{CO}$ ,  $\text{CO}_2$ , and  $\text{H}_2\text{O}$  in the optically thin limit [37]. The codes are coupled with Chemkin [39] and the Sandia transport [40] subroutine libraries. Several key binary diffusion coefficients involving atomic and molecular hydrogen are based on recent revisions [41,42].

In a recent study by Ji et al. [24], the axial velocity gradient along the centerline at the burner exit, denoted as  $\alpha$ , was found to have a considerable effect on the numerical determination of  $K_{\text{ext}}$ . The  $\alpha$  values at different experimental conditions, related to different measurements of  $K_{\text{ext}}$  for premixed flames, are documented in Table 2. For  $K_{\text{ext}}$  of nonpremixed flames, the  $\alpha$  values were determined to be, on the average, 40% of the  $K_{\text{ext}}$ .

$S_u^0$  and  $K_{\text{ext}}$  were simulated using the JetSurF 1.0 kinetic model [31]. The model includes 194 species and 1459 reactions describing the pyrolysis and high-temperature oxidation kinetics of  $n$ -paraffins up to  $n\text{-C}_{12}\text{H}_{26}$ . Additional details and an extensive set of validation results for JetSurF 1.0 can be found in [31].

Table 2 Axial velocity gradients at burner exit  $\alpha$  ( $\text{s}^{-1}$ ) at state of extinction of premixed flames with  $D = L = 10$  mm

$\phi$	JP-7	JP-8	S-8	Shell-GTL	R-8
0.8	200 ± 10	190 ± 10	170 ± 10	180 ± 10	180 ± 10
0.9	260 ± 10	240 ± 10	290 ± 10	300 ± 10	320 ± 10
1.0	450 ± 20	450 ± 20	490 ± 20	500 ± 20	520 ± 20
1.1	550 ± 20	510 ± 20	530 ± 20	560 ± 20	590 ± 20
1.2	540 ± 20	520 ± 20	520 ± 20	530 ± 20	540 ± 20
1.3	500 ± 20	530 ± 20	580 ± 20	580 ± 20	590 ± 20
1.4	440 ± 20	460 ± 20	510 ± 20	530 ± 20	550 ± 20
1.5	270 ± 10	240 ± 10	280 ± 10	310 ± 10	340 ± 10

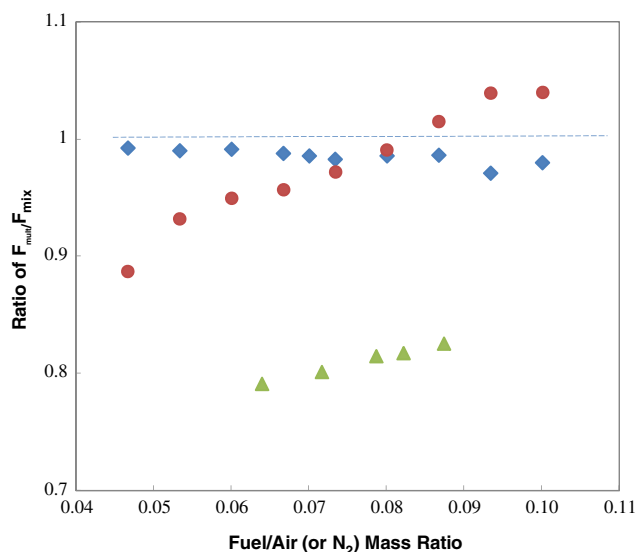


Fig. 5 Computed  $S_u^0$  (◆) and  $K_{\text{ext}}$  for premixed (●) and nonpremixed (▲) flames using the multicomponent transport formulation and scaled by the attendant values obtained using the mixture-averaged transport formulation.

Both the PREMIX and the opposed-jet codes allow for the use of either mixture-averaged or multicomponent formulations of transport coefficients. Figure 5 illustrates the differences between these two transport formulations in predicting  $S_u^0$  and  $K_{\text{ext}}$  for premixed and nonpremixed  $n\text{-C}_{12}\text{H}_{26}$  flames. It can be seen that, while the difference is less than 3% for  $S_u^0$ , for  $K_{\text{ext}}$ , it increases to more than 10 and 20% for premixed and nonpremixed flames, respectively. Thus, all the calculations in the present work were performed with the multicomponent transport formulation.

### IV. Results and Discussion

Figure 6 depicts the experimentally determined  $S_u^0$  of S-8/air, Shell-GTL/air, R-8/air, JP-7/air, and JP-8/air flames at  $T_u = 403$  K for  $0.7 \leq \phi \leq 1.5$  in this study, as well as experimental and computed  $S_u^0$  of  $n\text{-C}_{10}\text{H}_{22}$ /air and  $n\text{-C}_{12}\text{H}_{26}$ /air, as reported in [24] for the same thermodynamic conditions. The JetSurF 1.0 kinetic model closely predicts  $S_u^0$  of  $n\text{-C}_{10}\text{H}_{22}$ /air and  $n\text{-C}_{12}\text{H}_{26}$ /air mixtures within their experimental uncertainty.  $S_u^0$  of  $n$ -paraffin flames are the highest among all fuels. Compared with  $n$ -paraffins, S-8/air, Shell-GTL/air, and R-8/air flames exhibit similar  $S_u^0$ , while JP-7/air and JP-8/air flames propagate, on average, 5 and 8% slower, respectively. The maximum values of  $S_u^0$  are 62.7, 62.9, 62.8, 60.6, and 58.5 cm/s for S-8/air, Shell-GTL/air, R-8/air, JP-7/air, and JP-8/air flames, respectively, and they occur between  $\phi = 1.05$  to 1.1, similar to  $n$ -paraffin/air flames [24].

The relative magnitudes of  $S_u^0$  for flames of the various fuels is largely caused by differences in the oxidation kinetics of the different compounds present in jet fuels. Flames of alkylcycloparaffins and alkylbenzenes have lower  $S_u^0$  compared with  $n$ -paraffins (e.g., [43,44]). Equilibrium calculations show that alkylcycloparaffins/air and alkylbenzenes/air mixtures have either equal or higher adiabatic flame temperatures compared with  $n$ -paraffins/air flames. Thus, the observed differences in  $S_u^0$  are caused by kinetics. As shown in [43], during the initial reactions of alkylcycloparaffins, branched-chain intermediates are produced that subsequently crack to form large amounts of propene and allyl and less 1,3-butadiene compared with  $n$ -paraffins. Propene and allyl are less reactive compared with 1,3-butadiene, which constitutes an effective chain termination sequence [43]. Similarly, the initial reactions of alkylbenzenes [44], such as toluene or  $m$ -xylene, produce benzyl radicals that are relatively stable, the oxidation of which becomes a rate-limiting process for flame propagation. As shown in Table 1, JP-7 and JP-8 contain significant amounts of cycloparaffins and alkylbenzenes that tend to reduce the rate of flame propagation.

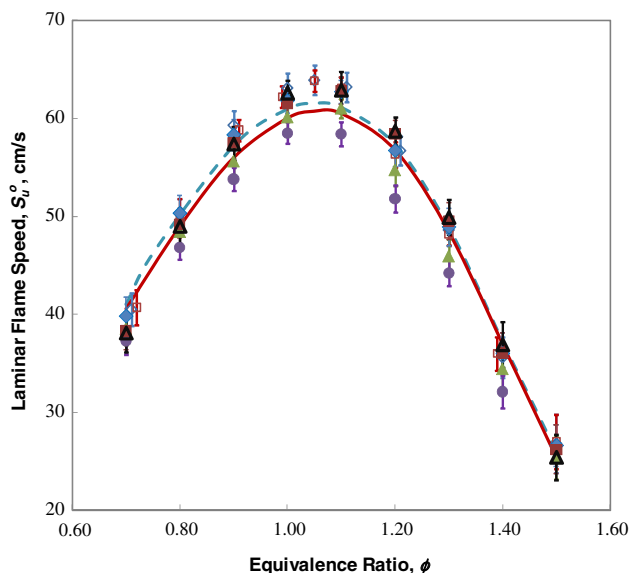


Fig. 6 Experimentally determined  $S_u^o$  at  $T_u = 403$  K of JP-7/air ( $\blacktriangle$ ), JP-8/air ( $\bullet$ ), S-8/air ( $\blacklozenge$ ), Shell-GTL/air ( $\triangle$ ), R-8/air ( $\blacksquare$ ),  $n$ -C<sub>10</sub>H<sub>22</sub>/air ( $\diamond$ ) [24], and  $n$ -C<sub>12</sub>H<sub>26</sub>/air ( $\square$ ) [24]; and computed  $S_u^o$  of  $n$ -C<sub>10</sub>H<sub>22</sub>/air (dashed line) and  $n$ -C<sub>12</sub>H<sub>26</sub>/air (solid line) mixtures using JetSurF 1.0 kinetic model.

Figure 7 depicts the experimentally determined  $K_{\text{ext}}$  of premixed S-8/air, Shell-GTL/air, R-8/air, JP-7/air, and JP-8/air flames as functions of  $\phi$ , along with previously reported  $K_{\text{ext}}$  of  $n$ -C<sub>10</sub>H<sub>22</sub>/air and  $n$ -C<sub>12</sub>H<sub>26</sub>/air flames [24]. Similar to  $S_u^o$ , R-8, Shell-GTL, S-8,  $n$ -C<sub>10</sub>H<sub>22</sub>, and  $n$ -C<sub>12</sub>H<sub>26</sub> flames exhibit similar resistance to extinction. Compared with S-8/air, Shell-GTL/air, and R-8/air flames,  $K_{\text{ext}}$  of JP-7/air and JP-8/air flames are lower. As mentioned earlier, the observed ranking of the extinction propensity is caused largely by the differences in the oxidation kinetics of the different fuels considered in this study. Another observation is that the peak values of  $K_{\text{ext}}$  for all the flames occur around  $\phi = 1.2$ , which is greater than the attendant value for  $S_u^o$ . This is largely due to the increase of flame temperature at positive stretch for subunity Lewis numbers  $Le$ , as is the case for fuel-rich mixtures (e.g., [26]).

Figure 8 depicts the experimental  $K_{\text{ext}}$  as functions of fuel/ $N_2$  mass ratio ( $(F/N_2)_{\text{mass}}$ ) for nonpremixed flames of  $n$ -C<sub>10</sub>H<sub>22</sub>,

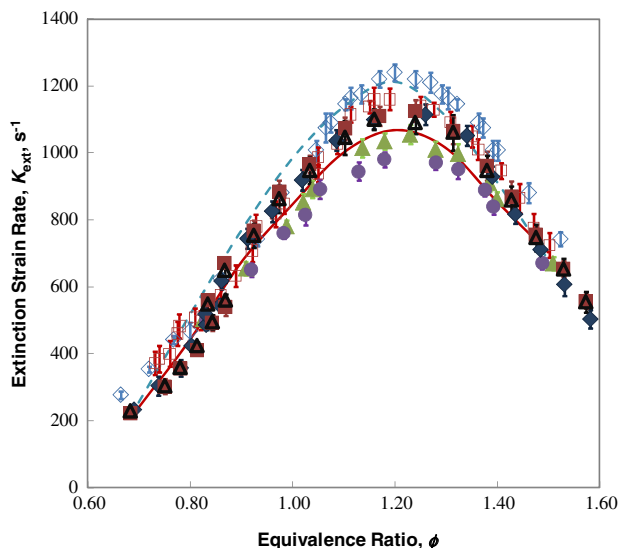


Fig. 7 Experimentally determined  $K_{\text{ext}}$  at  $T_u = 403$  K of JP-7/air ( $\blacktriangle$ ), JP-8/air ( $\bullet$ ), S-8/air ( $\blacklozenge$ ), Shell-GTL/air ( $\triangle$ ), R-8/air ( $\blacksquare$ ),  $n$ -C<sub>10</sub>H<sub>22</sub>/air ( $\diamond$ ) [24], and  $n$ -C<sub>12</sub>H<sub>26</sub>/air ( $\square$ ) [24]; and computed  $K_{\text{ext}}$  of  $n$ -C<sub>10</sub>H<sub>22</sub>/air (dashed line) and  $n$ -C<sub>12</sub>H<sub>26</sub>/air (solid line) using JetSurF 1.0 kinetic model.

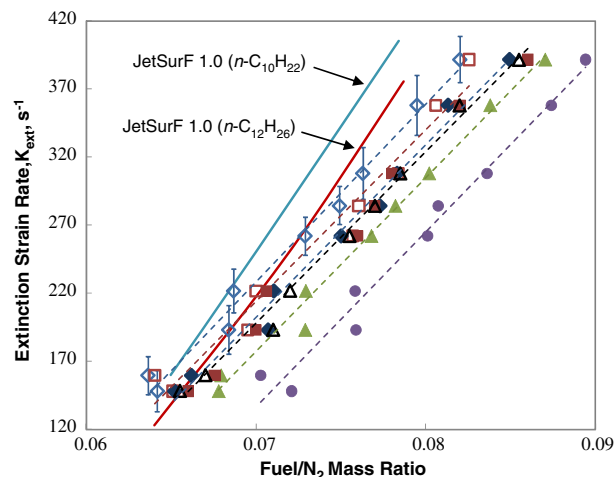


Fig. 8 Experimental  $K_{\text{ext}}$  of  $n$ -C<sub>10</sub>H<sub>22</sub>/ $N_2$  ( $\diamond$ ),  $n$ -C<sub>12</sub>H<sub>26</sub>/ $N_2$  ( $\square$ ), JP-7/ $N_2$  ( $\blacktriangle$ ), JP-8/ $N_2$  ( $\bullet$ ), S-8/ $N_2$  ( $\blacklozenge$ ), Shell-GTL/ $N_2$  ( $\triangle$ ), and R-8/ $N_2$  ( $\blacksquare$ ) nonpremixed flames; and computed  $K_{\text{ext}}$  using the JetSurF 1.0 model (solid lines) and best fit of the experimental data (dashed lines).

$n$ -C<sub>12</sub>H<sub>26</sub>, JP-7, JP-8, S-8, Shell-GTL, and R-8; in all experiments, the oxidizer was  $O_2$ . The computed results of  $n$ -C<sub>10</sub>H<sub>22</sub>/ $N_2$  and  $n$ -C<sub>12</sub>H<sub>26</sub>/ $N_2$  are indicated with solid lines, and they were performed using the JetSurF 1.0 model. The experimental data were fitted using dashed lines to facilitate the comparisons. Only the uncertainties of the  $n$ -C<sub>10</sub>H<sub>22</sub>/ $N_2$  flames are shown for clarity, and they are similar for all flames considered. Among all fuels,  $n$ -C<sub>10</sub>H<sub>22</sub> flames have the highest resistance to extinction, followed by  $n$ -C<sub>12</sub>H<sub>26</sub> (S-8, Shell-GTL, and R-8), JP-7, and JP-8 flames, in descending order. Compared with flame propagation and extinction of premixed flames, the nonpremixed flame results reveal more discriminative differences in the extinction behavior among the fuels, although there are no distinguishable differences among the S-8, Shell-GTL, and R-8 flames. For example, JP-8/air mixtures propagate 8% slower than  $n$ -C<sub>10</sub>H<sub>22</sub>/air mixtures, while this difference increases to 25% when comparing  $K_{\text{ext}}$  of the corresponding nonpremixed flames. This is reasonable, because kinetics and reactant diffusion affect the extinction of nonpremixed flames in a more profound way (e.g., [45]). It is also noted that the JetSurF 1.0 model overpredicts  $K_{\text{ext}}$  of nonpremixed  $n$ -C<sub>10</sub>H<sub>22</sub>/ $N_2$  and  $n$ -C<sub>12</sub>H<sub>26</sub>/ $N_2$  mixtures by as much as 10%. On the other hand, JetSurF 1.0 slightly underpredicts  $S_u^o$  (Fig. 6) and  $K_{\text{ext}}$  of premixed flames (Fig. 7). This is largely due to the uncertainties associated with the reactant diffusion coefficients, which have a greater effect on nonpremixed flames compared with premixed flames.

To provide insight into the first-order effects on the combustion behavior of jet fuels, numerical simulations and attendant sensitivity analyses were carried out for  $n$ -C<sub>12</sub>H<sub>26</sub> flames. Figures 9 and 10 depict the ranked logarithmic sensitivity coefficients of  $S_u^o$  and  $K_{\text{ext}}$  on kinetics and binary diffusion coefficients, respectively. The sensitivity results are presented for stoichiometric flame and a  $(\text{fuel}/N_2)_{\text{mass}} = 0.066$  nonpremixed flame.

The results of Fig. 9 reveal that, compared with  $S_u^o$ ,  $K_{\text{ext}}$  for premixed flames is notably more sensitive to kinetics. The reason is that  $K_{\text{ext}} \sim \omega$ , while  $S_u^o \sim (\omega)^{1/2}$ , where  $\omega$  is the overall reaction rate [46]. The sensitivity of  $K_{\text{ext}}$  to kinetics appears to be different under premixed and nonpremixed conditions. This is largely due to the locations at which key reactions, such as the main branching  $H + O_2 \rightarrow OH + O$  and main termination  $H + O_2 + M \rightarrow HO_2 + M$ , take place and the directions of diffusive transport of key species in the two different reacting configurations.

The results of Fig. 10 reveal that both  $S_u^o$  and  $K_{\text{ext}}$  are rather sensitive to the  $O_2 - N_2$  binary diffusion coefficient. For fuel-lean or stoichiometric premixed flames, increasing the diffusivity of  $O_2$  results in higher flux of  $O_2$  into the reaction zone, which makes the flame more fuel-lean and less reactive, resulting in lower  $S_u^o$  and  $K_{\text{ext}}$ . In nonpremixed flames, however, increasing the diffusivity of  $O_2$  increases the efficiency of diffusion of  $O_2$  toward the fuel side, thus

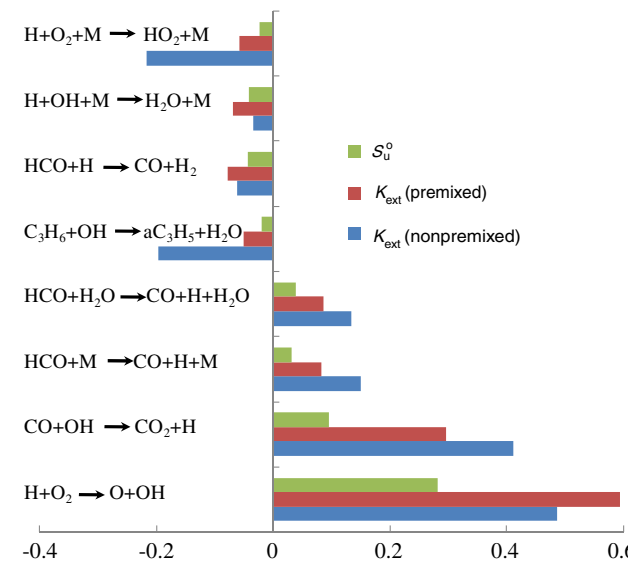


Fig. 9 Ranked logarithmic sensitivity coefficients on kinetics of  $S_u^0$  and  $K_{ext}$  for a stoichiometric  $n$ -C<sub>12</sub>H<sub>26</sub>/air flame, and of  $K_{ext}$  of a  $(n$ -C<sub>12</sub>H<sub>26</sub>/N<sub>2</sub>)<sub>mass</sub> = 0.066 nonpremixed flame.

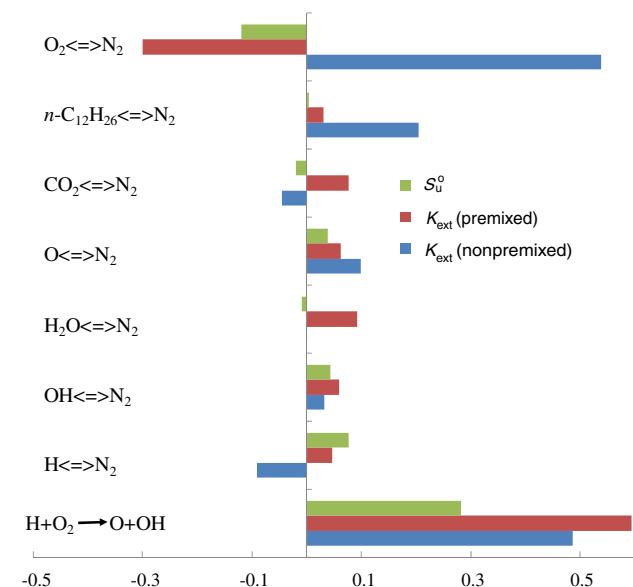


Fig. 10 Ranked logarithmic sensitivity coefficients on binary diffusion coefficients of  $S_u^0$  and  $K_{ext}$  for a stoichiometric  $n$ -C<sub>12</sub>H<sub>26</sub>/air flame, and of  $K_{ext}$  of a  $(n$ -C<sub>12</sub>H<sub>26</sub>/N<sub>2</sub>)<sub>mass</sub> = 0.066 nonpremixed flame. The sensitivity on the main branching reaction is also shown for comparison.

augmenting the rate of the main branching reaction  $H + O_2 \rightarrow O + OH$  and increasing the resistance to extinction. Also, the binary diffusion coefficients of H, O, and OH radicals in N<sub>2</sub> exhibit positive influence on  $K_{ext}$  of premixed flames. However, this is not the case for the  $H - N_2$  binary diffusion coefficient for nonpremixed flames. Larger diffusivity of H leads to greater losses of H from the reaction zone upstream and into the fuel/N<sub>2</sub> stream, thus retarding the overall reactivity. The diffusion of  $n$ -C<sub>12</sub>H<sub>26</sub> to N<sub>2</sub> has no significant effect on  $S_u^0$  but has a notable effect on  $K_{ext}$  for nonpremixed flames. Thus, for the near-extinction nonpremixed flames considered in this investigation, the overall reaction is limited by the transport of fuel toward the reaction zone.

## V. Conclusions

Laminar flame speeds and extinction strain rates of premixed S-8/air, Shell-GTL/air, R-8/air, JP-7/air, and JP-8/air flames were determined experimentally as functions of fuel/air mass ratio at an

elevated unburned mixture temperature and atmospheric pressure. Extinction strain rates of nonpremixed flames of S-8, Shell-GTL, R-8, JP-7, JP-8,  $n$ -decane, and  $n$ -dodecane/air were determined experimentally as well. Results revealed that the propagation rates of S-8/air, Shell-GTL/air, and R-8/air flames are similar to those of  $n$ -decane/air and  $n$ -dodecane/air, while JP-7/air and JP-8/air flames propagate at rates that are 5 and 8% lower, respectively. Similarly, JP-7 and JP-8 flames were found to be less resistant to extinction compared with  $n$ -decane,  $n$ -dodecane, S-8, Shell-GTL, and R-8 flames under both premixed and nonpremixed conditions. This effect is caused largely by differences in the oxidation kinetics of the different classes of hydrocarbon compounds that are present in these fuels. There is no distinguishable difference found between bioderived jet fuel (R-8) and F-T processed jet fuels (S-8 and Shell-GTL) in the present study. Sensitivity analysis also revealed that, compared with flame propagation, flame extinction is, in general, more sensitive to kinetics and diffusion, especially under nonpremixed conditions.

It is of interest to note that the laminar flame speeds, a measure of the heat release rate, of  $n$ -decane and  $n$ -dodecane flames closely reproduce those of the alternative fuels and are within 5–8% compared with JP-7 and JP-8 flames. Thus, heat release rates resulting from  $n$ -decane and  $n$ -dodecane flames can be used to approximate to the first order those of real jet fuels. However, it should be noted that such one-component surrogates might not be able to mimic other combustion properties of real jet fuels including extinction and ignition.

## Acknowledgment

The work was sponsored by the U.S. Air Force Office of Scientific Research (grant numbers FA9550-07-1-0168 and FA9550-08-1-0040) under the technical supervision of Julian M. Tishkoff.

## References

- [1] Edwards, T., "Liquid Fuels and Propellants for Aerospace Propulsion," *Journal of Propulsion and Power*, Vol. 19, No. 6, 2003, pp. 1089–1107. doi:10.2514/2.6946
- [2] Edwards, T., Minus, D., Harrison, W., Corporan, E., DeWitt, M., Zabarnick, S., and Balster, L., "Fischer-Tropsch Jet Fuels: Characterisation for Advanced Aerospace Applications," 40th Joint Propulsion Conference and Exhibit, Fort Lauderdale, FL, AIAA Paper 2004-3885, July 2004.
- [3] Huber, M. L., Smith, B. L., Ott, L. S., and Bruno, T. J., "Surrogate Mixture Model for the Thermophysical Properties of Synthetic Aviation Fuel S-8: Explicit Application of the Advanced Distillation Curve," *Energy and Fuels*, Vol. 22, No. 2, 2008, pp. 1104–1114. doi:10.1021/ef700562c7
- [4] Colket, M., Edwards, T., Williams, S., Cernansky, N. P., Miller, D. L., Egolopoulos, F. N., Lindstedt, P., Seshadri, K., Dryer, F. L., Law, C. K., Friend, D., Lenhart, D. B., Pitsch, H., Sarofim, A., Smooke, M., and Tsang, W., "Development of an Experimental Database and Kinetic Models for Surrogate Jet Fuels," 45th AIAA Aerospace Sciences Meeting and Exhibit, Reno, NV, AIAA Paper 2007-0770, 2007.
- [5] Mawid, M. A., Park, T. W., Sekar, B., and Arana, C., "Development and Validation of a Detailed JP-8 Fuel Chemistry Mechanism," 38th Joint Propulsion Conference and Exhibit, Indianapolis, IN, AIAA Paper 2002-3876, July 2002.
- [6] Lenhart, D. B., Miller, D. L., and Cernansky, N. P., "The Oxidation of JP-8, Jet-A, and Their Surrogates in the Low and Intermediate Temperature Regime at Elevated Pressures," *Combustion Science and Technology*, Vol. 179, No. 5, 2007, pp. 845–861. doi:10.1080/00102200600672011
- [7] Vasu, S. S., Davidson, D. F., and Hanson, R. K., "Jet Fuel Ignition Delay Times: Shock Tube Experiments over Wide Conditions and Surrogate Model Predictions," *Combustion and Flame*, Vol. 152, Nos. 1–2, 2008, pp. 125–143. doi:10.1016/j.combustflame.2007.06.019
- [8] Davidson, D. F., Haylett, D. R., and Hanson, R. K., "Development of an Aerosol Shock Tube for Kinetic Studies of Low-Vapor-Pressure Fuels," *Combustion and Flame*, Vol. 155, Nos. 1–2, 2008, pp. 108–117. doi:10.1016/j.combustflame.2008.01.006
- [9] Eisazadeh-Far, K., Parsinejad, F., and Metghalchi, H., "Flame Structure and Laminar Burning Speeds of JP-8/Air Premixed Mixtures at High

- Temperatures and Pressures," *Fuel*, Vol. 89, No. 5, 2010, pp. 1041–1049.  
doi:10.1016/j.fuel.2009.11.032
- [10] Humer, S., Frassoldati, A., Granata, S., Faravelli, T., Ranzi, E., Seiser, R., and Seshadri, K., "Experimental and Kinetic Modeling Study of Combustion of JP-8, Its Surrogates and Reference Components in Laminar Nonpremixed Flows," *Proceedings of the Combustion Institute*, Vol. 31, No. 1, 2007, pp. 393–400.  
doi:10.1016/j.proci.2006.08.008
  - [11] Convery, J. L., Pellett, G. L., O'Brien, W. F., and Wilson, L. G., "An Experimental Study of *n*-Heptane and JP-7 Extinction Limits in an Opposed Jet Burner," 41st Joint Propulsion Conference and Exhibit, Tucson, AZ, AIAA Paper 2005-3776, July 2005.
  - [12] Holley, A. T., Dong, Y., Andac, M. G., Egolfopoulos, F. N., and Edwards, T., "Ignition and Extinction of Non-Premixed Flames of Single-component Liquid Hydrocarbons, Jet Fuels, and Their Surrogates," *Proceedings of the Combustion Institute*, Vol. 31, No. 1, 2007, pp. 1205–1213.  
doi:10.1016/j.proci.2006.07.208
  - [13] Dattarajan, S., Park, O., Fisher, E. M., and Gouldin, F. C., "Subatmospheric Extinction of Opposed-Jet Diffusion Flames of Jet Fuel and Its Surrogates," *AIAA Journal*, Vol. 48, No. 1, 2010, pp. 158–165.  
doi:10.2514/1.42742
  - [14] Kumar, K., Sung, C. J., and Hui, X., "Laminar Flame Speeds and Extinction Limits of Conventional and Alternative Jet Fuels," 47th AIAA Aerospace Sciences Meeting, Orlando, FL, AIAA Paper 2009-991, Jan. 2009.
  - [15] Puri, P., Ma, R., Choi, J., and Yang, V., "Ignition Characteristics of Cracked JP-7 Fuel," *Combustion and Flame*, Vol. 142, No. 4, 2005, pp. 454–457.  
doi:10.1016/j.combustflame.2005.06.001
  - [16] Lindstedt, R. P., and Maurice, L. Q., "Detailed Chemical-Kinetic Model for Aviation Fuels," *Journal of Propulsion and Power*, Vol. 16, No. 2, 2000, pp. 187–195.  
doi:10.2514/2.5582
  - [17] Dagaut, P., and Cathonnet, M., "The Ignition, Oxidation, and Combustion of Kerosene: A Review of Experimental and Kinetic Modeling," *Progress in Energy and Combustion Science*, Vol. 32, 2006, pp. 48–92.  
doi:10.1016/j.peccs.2005.10.003
  - [18] Ranzi, E., Frassoldati, A., Granata, S., and Faravelli, T., "Wide-Range Kinetic Modeling Study of the Pyrolysis, Partial Oxidation, and Combustion of Heavy *n*-Alkanes," *Industrial and Engineering Chemistry Research*, Vol. 44, No. 14, 2005, pp. 5170–5183.  
doi:10.1021/ie049318g
  - [19] Zhang, H. R., Eddings, E. G., and Sarofim, A. F., "Criteria for Selection of Components for Surrogates of Natural Gas and Transportation Fuels," *Proceedings of the Combustion Institute*, Vol. 31, No. 1, 2007, pp. 401–409.  
doi:10.1016/j.proci.2006.08.001
  - [20] Violi, A., Yan, S., Eddings, E. G., Sarofim, A. F., Granata, S., Faravelli, T., and Ranzi, E., "Experimental Formulation and Kinetic Model for JP-8 Surrogate Mixtures," *Combustion Science and Technology*, Vol. 174, No. 11, 2002, pp. 399–417.  
doi:10.1080/00102200215080
  - [21] Cooke, J. A., Bellucci, M., Smooke, M. D., Gomez, A., Violi, A., Favarelli, T., and Ranzi, E., "Computational and Experimental Study of JP-8, a Surrogate, and Its Components in Counterflow Diffusion Flames," *Proceedings of the Combustion Institute*, Vol. 30, No. 1, 2005, pp. 439–446.  
doi:10.1016/j.proci.2004.08.046
  - [22] Agostaa, A., Cernanskya, N. P., Millera, D. L., Faravellib, T., and Ranzi, E., "Reference Components of Jet Fuels: Kinetic Modeling and Experimental Results," *Experimental Thermal and Fluid Science*, Vol. 28, No. 7, 2004, pp. 701–708.  
doi:10.1016/j.expthermflusci.2003.12.006
  - [23] Dooley, S., Won, S. H., Chaos, M., Heyne, J., Ju, Y., Dryer, F. L., Kumar, K., Sung, C. J., Wang, H., Oehlschlaeger, M. A., Santoro, R. J., and Litzinger, T. A., "A Jet Fuel Surrogate Formulated by Real Fuel Properties," *Combustion and Flame*, Vol. 157, No. 12, 2010, pp. 2333–2339.  
doi:10.1016/j.combustflame.2010.07.001
  - [24] Ji, C., Dames, E., Wang, Y. L., Wang, H., and Egolfopoulos, H., "Propagation and Extinction of Premixed C5–C12 *n*-Alkane Flames," *Combustion and Flame*, Vol. 157, No. 2, 2010, pp. 277–287.  
doi:10.1016/j.combustflame.2009.06.011
  - [25] Wu, C. K., and Law, C. K., "On the Determination of Laminar Flame Speeds from Stretched Flames," *Proceedings of the Combustion Institute*, Vol. 20, No. 1, 1984, pp. 1941–1949.  
doi:10.1016/S0082-0784(85)80693-7
  - [26] Law, C. K., Zhu, D. L., and Yu, G., "Propagation and Extinction of Stretched Premixed Flames," *Proceedings of the Combustion Institute*, Vol. 21, No. 1, 1986, pp. 1419–1426.  
doi:10.1016/S0082-0784(88)80374-6
  - [27] Zhu, D. L., Egolfopoulos, F. N., and Law, C. K., "Experimental and Numerical Determination of Laminar Flame Speeds of Methane/(Ar, N<sub>2</sub>, CO<sub>2</sub>)-Air Mixtures as Function of Stoichiometry, Pressure, and Flame Temperature," *Proceedings of the Combustion Institute*, Vol. 22, No. 1, 1988, pp. 1537–1545.  
doi:10.1016/S0082-0784(89)80164-X
  - [28] Holley, A. T., Dong, Y., Andac, M. G., and Egolfopoulos, F. N., "Extinction of Premixed Flames of Practical Liquid Fuels: Experiments and Simulations," *Combustion and Flame*, Vol. 144, No. 3, 2006, pp. 448–460.  
doi:10.1016/j.combustflame.2005.08.001
  - [29] Wang, Y. L., Holley, A. T., Ji, C., Egolfopoulos, F. N., Tsotsis, T. T., and Curran, H. J., "Propagation and Extinction of Premixed Dimethyl-Ether/Air Flames," *Proceedings of the Combustion Institute*, Vol. 32, No. 1, 2009, pp. 1035–1042.  
doi:10.1016/j.proci.2008.06.054
  - [30] Veloo, P. S., Wang, Y. L., Egolfopoulos, F. N., and Westbrook, C. K., *Combustion and Flame*, Vol. 157, No. 10, 2010, pp. 1989–2004.  
doi:10.1016/j.combustflame.2010.04.001
  - [31] Sirjean, B., Dames, E., Sheen, D. A., You, X.-Q., Sung, C., Holley, A. T., Egolfopoulos, F. N., Wang, H., Vasu, S. S., Davidson, D. F., Hanson, R. K., Pitsch, H., Bowman, C. T., Kelley, A., Law, C. K., Tsang, W., Cernansky, N. P., Miller, D. L., Violi, A., and Lindstedt, R. P., "A High-Temperature Chemical Kinetic Model of *n*-Alkane Oxidation, JetSurF Version 1.0," <http://melchior.usc.edu/JetSurF/JetSurF1.0/Index.html> [retrieved 15 Sept. 2009].
  - [32] Wernet, M. P., "A Flow Field Investigation in the Diffuser of a High-speed Centrifugal Compressor Using Digital Particle Imaging Velocimetry," *Measurement Science and Technology*, Vol. 11, No. 7, 2000, pp. 1007–1022.  
doi:10.1088/0957-0233/11/7/316
  - [33] Salicone, S., *Measurement Uncertainty: An Approach via the Mathematical Theory of Evidence*, 1st ed., Springer Science and Business Media, New York, 2006, Chap. 1.4.
  - [34] Bowerman, B. L., and O'Connell, R. T., *Linear Statistical Models: An Applied Approach*, 2nd ed., PWS-Kent, Boston, 1990, Chap. 5.6.
  - [35] Kee, R. J., Grcar, J. F., Smooke, M. D., and Miller, J. A., "A FORTRAN Program for Modeling Steady Laminar One-Dimensional Premixed Flames," Sandia National Labs., Rept. SAND85-8240, Livermore, CA, 1985.
  - [36] Grcar, J. F., Kee, R. J., Smooke, M. D., and Miller, J. A., "A Hybrid Newton/Time-Integration Procedure for the Solution of Steady, Laminar, One-Dimensional, Premixed Flames," *Proceedings of the Combustion Institute*, Vol. 21, 1986, pp. 1773–1782.  
doi:10.1016/S0082-0784(88)80411-9
  - [37] Egolfopoulos, F. N., "Geometric and Radiation Effects on Steady and Unsteady Strained Laminar Flames," *Proceedings of the Combustion Institute*, Vol. 25, 1994, pp. 1375–1381.  
doi:10.1016/S0082-0784(06)80780-0
  - [38] Kee, R. J., Miller, J. A., Evans, G. H., and Dixon-Lewis, G., "A Computational Model of the Structure and Extinction of Strained, Opposed Flow, Premixed Methane-Air Flames," *Proceedings of the Combustion Institute*, Vol. 22, 1988, pp. 1479–1494.  
doi:10.1016/S0082-0784(89)80158-4
  - [39] Kee, R. J., Rupley, F. M., and Miller, J. A., "Chemkin-II: A FORTRAN Chemical Kinetics Package for the Analysis of Gas-Phase Chemical Kinetics," Sandia National Labs., Rept. SAND89-8009, Livermore, CA, 1989.
  - [40] Kee, R. J., Warnatz, J., and Miller, J. A., "A FORTRAN Computer Code Package for the Evaluation of Gas-Phase Viscosities, Conductivities, and Diffusion Coefficients," Sandia National Labs., Rept. SAND83-8209, Livermore, CA, 1983.
  - [41] Dong, Y., Holley, A. T., Andac, M. G., Egolfopoulos, F. N., Davis, S. G., Middha, P., and Wang, H., "Extinction of Premixed H<sub>2</sub>/Air Flames: Chemical Kinetics and Molecular Diffusion Effects," *Combustion and Flame*, Vol. 142, No. 4, 2005, pp. 374–387.  
doi:10.1016/j.combustflame.2005.03.017
  - [42] Middha, P. and Wang, H., "First-principle Calculation for the High-temperature Diffusion Coefficients of Small Pairs: the H-Ar Case," *Combustion Theory and Modelling*, Vol. 9, No. 2, 2005, pp. 353–363.  
doi:10.1080/13647830500098431
  - [43] Ji, C., Dames, E., Sirjean, B., Wang, H., and Egolfopoulos, F. N., "An Experimental and Modeling Study of the Propagation of Cyclohexane

- and Mono-Alkylated Cyclohexane Flames,” *Proceedings of the Combustion Institute*, Vol. 33, No. 1, 2011, pp. 971–978.  
doi:10.1016/j.proci.2010.06.099
- [44] Ji, C., Moheet, A., Wang, Y. L., Colket, M., Wang, H., and Egolfopoulos, F. N., “An Experimental Study of Premixed *m*-Xylene/Air and *n*-Dodecane/*m*-Xylene/Air Flames,” *6th U.S. Combustion Meeting*, Ann Arbor, MI, Central States Section of the Combustion Institute Paper 31H2, Pittsburgh, PA, May 2009.
- [45] Holley, A. T., You, X. Q., Dames, E., Wang, H., and Egolfopoulos, F. N., “Sensitivity of Propagation and Extinction of Large Hydrocarbon Flames to Fuel Diffusion,” *Proceedings of the Combustion Institute*, Vol. 32, No. 1, 2009, pp. 1157–1163.  
doi:10.1016/j.proci.2008.05.067
- [46] Law, C. K., *Combustion Physics*, 1st ed., Cambridge Univ. Press, New York, 2006, Chap. 10.2, pp. 410–411.

L. Maurice  
Associate Editor